Morphological Modeling and Deformation of 3D Objects

by

Samuel Boivin*, André Gagalowicz* and Youichi Horry**

***Mirages Project,** I.N.R.I.A. Rocquencourt,

Domaine de Voluceau, 78153 Le Chesnay Cedex, France

{Samuel.Boivin|Andre.Gagalowicz}@inria.fr,

**** Hitachi,** Central Research Laboratory,

1-280 Higashi-Koigakubo, Kokubunji-shi, Tokyo 185 Japan

horry@crl.hitachi.co.jp

ABSTRACT

This paper describes a new set of techniques based upon laws of object composition for the modeling and animation of deformable objects. They present some similarities with logical or morphological operations. This method is unique because the volume of the merged object is held constant with respect to its constituents. Composition from two objects is allowed for general shapes which may have very different topologies. These techniques are applied towards shapes which are approximated by a polyhedral description. When integrated into a modeler, they can be used as modeling tools, animation tools, deformation tools or even morphing tools depending on how they are handled. One of the advantages of these tools is that the user may easily deduce the procedure to follow in order to obtain a given result.

1 INTRODUCTION

Deformable objects are useful to make striking animations (i.e. human form merged with a creature's body, liquids, many solid objects...). In the real world, such objects may be considered as incompressible. Animators of 2D cel animations are always taking care of volume conservation in their drawings. Many techniques were proposed for modeling and animating such 3D deformable objects [1, 3, 4, 10, 11, 13, 14, 15, 17], but

they are not designed to control volume conservation. On the other hand, non deformable objects (i.e. robots, mechanical ones...) are rather easy to animate; we have just to translate and rotate the parts of the objects. In this paper, we propose a new method which is able to model and animate deformable objects. We keep the total volume of the objects constant (i.e. we suppose that they are incompressible).

Volume preserving deformations could be convenient in the design of packaging containers which must have a precise volume such as perfume bottles and could provide relatively a simple tool for animating objects such as limbs and prostethic devices which can be deformed while bending. These tools could also be useful in industrial design where one could explore the variety of deformations possible on a fixed volume of raw material. It produces a clay modeler in essence (see figure 0) which could be used as such in a graphical modeling system.

The techniques presented can easily be generalized to mass conservation by using appropriate normalization factors for the combined objects. Volume control during object deformation could also have applications in biology for the qualitative visualization of models such as cell division (mitosis) and cell fusion (lymphocyte function).

One can conserve volume but it is also easy to allow a tunable degree of incompressibility simply be changing Eq (1) to include an extra scaling factor . This way, one can control the degree of stretching which could be useful in the development of compressible models that could be used for visualizing cardiac function, etc...

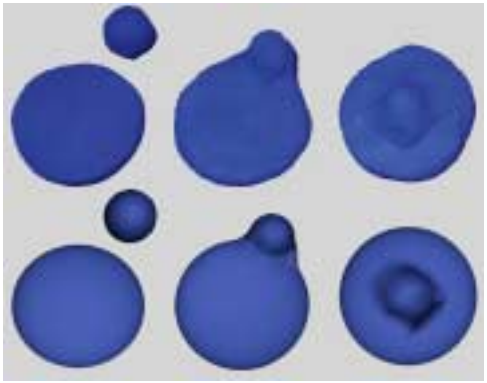

Figure 0: Fusion of two natural clay shapes (top) and simulation of this fusion using our techhnique (bottom)

1.1 Previous Work

Many techniques have been already developed to create and animate complex objects. Using the composition of simple primitives, more complex objects can be obtained; for example using metaballs ([19], [22], [23]) or CSG ([20], [24], [25]). Surfaces of smooth shapes can be generated by patches such as B-splines ([3], [1]). They can be approximated by a vertex/edge/facet network which allows them to be mixed with surfaces obtained by other methods. By moving control points of the patches, surfaces can be readily animated. Implicit surfaces are another way to create and animate smooth shapes. They can simulate smooth fusions between objects([13], [14], [15]). A different manner of constructing a complex shape is to deform a preexisting one with a given deformation tool (Free-Form Deformations [11], [4]). Then, the tool can be animated (Animated Free-Form Deformation [8]). Interesting animated shapes may also be obtained through the metamorphosis from one shape to another one ([7], [10], [21]) or by using composition laws between two shapes. As an example, in reference 9, the Minkovski sum between two object shapes is computed.

Another technique which is closely related to this work allows the composition of two interpenetrating shapes when one of the objects is a star-shaped [16].

1.2 *Current Approach*

We introduce what we call “morphological” modeling operators. The two basic morphological modeling operators consist of the “fusion” and the “difference” operators which correspond to erosion and dilation in mathematical morphology. The fusion operator generates an object with a volume which is equal to the sum of the volumes of two input objects. The difference operator generates an object with a volume which is equal to the difference between the volumes of the two. Using a combination of both operators, we demonstrate how to deform objects while keeping their volume constant. These new deformation tools are called morphological deformation operators. One goal is to easily animate deformable objects. To achieve this, we use preexisting 3D shapes and animate (i.e. translate and rotate) them. Then at each frame we dispose of the

locations of the various objects that we compose by any combination of morphological modeling operators. Various applications of the volume preverving operators are shown in Figures 1-6.

On Figure 1, we show the composition of two shapes, the result of which, called fusion, is such that the result object contains the union of A and B, and has a volume equal to the sum of volume of A and B. This shape seems more appealing than the union of the two objects (left of Figure 1).

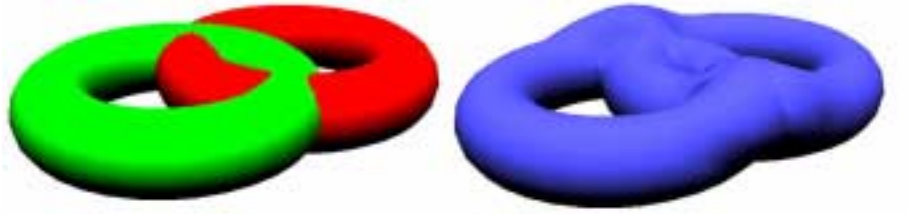

Figure 1: Fusion of two toruses (the two input toruses are shown respectively in green and red, and the result of fusion in blue)

On Figure 2, the difference between A and B is such that the result volume is equal to the difference of the two volumes, and contains the logical difference between A and B.

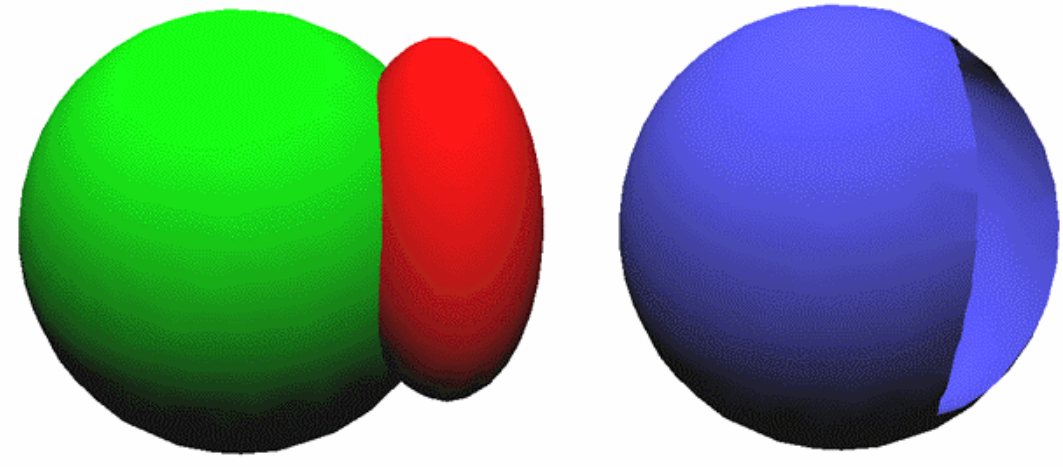

Figure 2: Difference between Object A (green) and Object B (red), presented in blue

On Figure 3, object B (in red) is used to deform object A (green) is such a way that the volume of A remains constant, but the deformation produced is monitored by the shape of B.

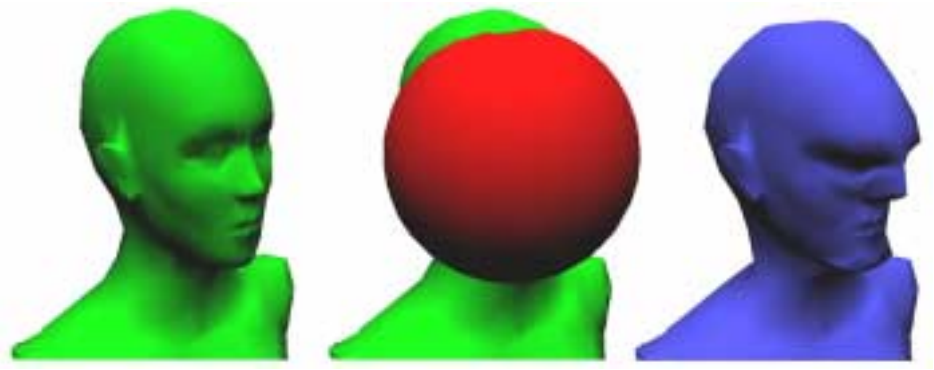

Figure 3: Attraction of Object A (green) by Object B (red), shown in blue

On Figure 4, object B is used to repell object A, but the deformation produced, once again, does not change the volume of A.

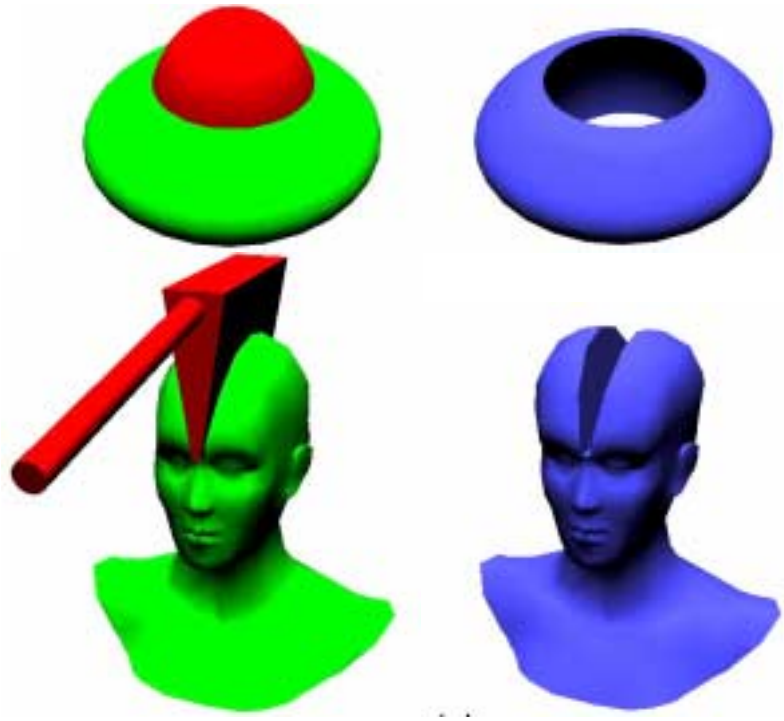

Figure 4: Repulsion of Object A (green) by Object B (red), shown in blue

On Figure 5, object B is filled up by a part of the volume of A, and then separated from A. The resulting volume of A is equal to the difference between the original volume of A and the volume of B.

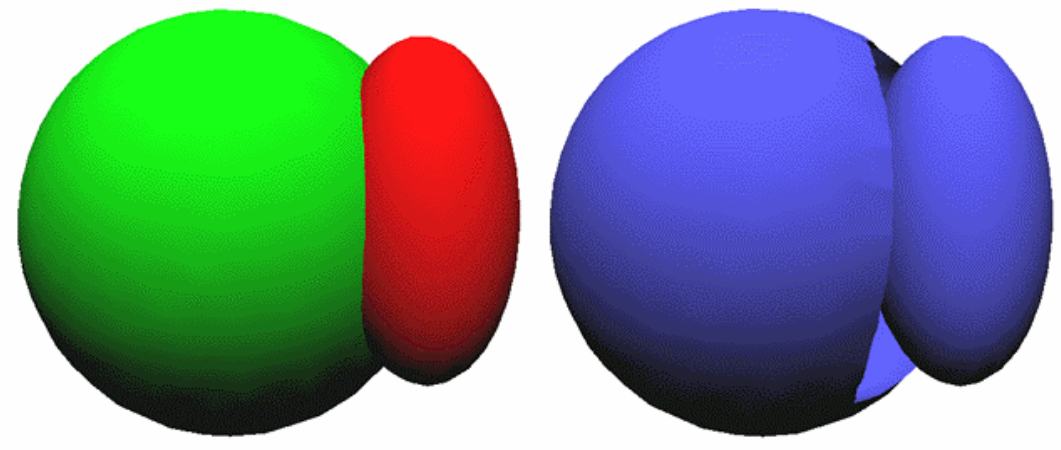

Figure 5: Separation of Object A (green) by Object B (red), in blue

Figure 6 presents several images corresponding to the morphing of a single sphere onto a set of five disjoint spheres (very different topology). Morphing is performed automatically in 3D, and the volume of the morphed object varies linearly during the sequence.

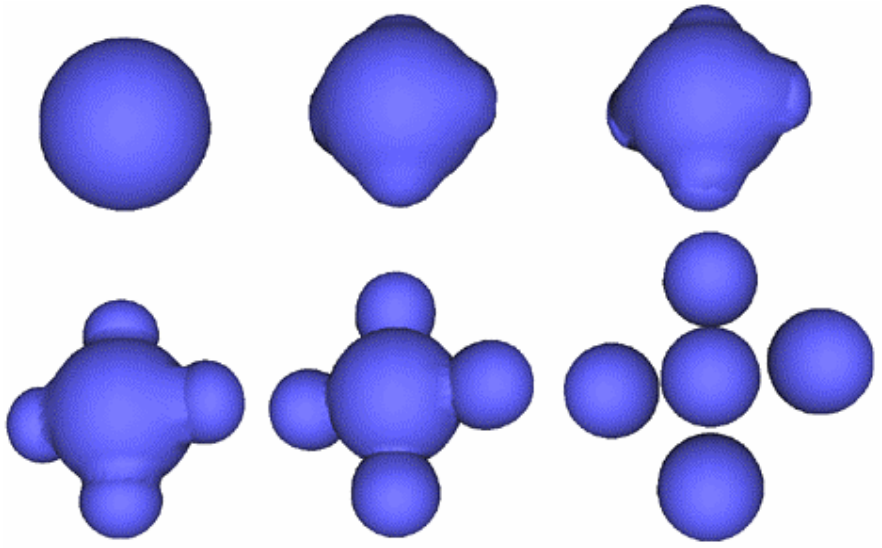

Figure 6: 3D Morphing from a single sphere to five ones

Let us give now a more precise definition of these various operators, presented above.

- **the fusion**

the fusion of two objects is such that the fused objects have a volume equal to the sum of the two initial volumes (close to a logical union in CSG).

- **the difference**

The difference between two objects produces another one which has a volume equal to the difference between the two former volumes (negative volumes are allowed, corresponding to their existence in a negative world as in Astrophysics). This difference is close to what we obtain when we compute the intersection between two objects and suppress it from them. More precisely, when we consider the difference between A and B, we suppose that A has a positive mass, B, a negative one; if they come to contact, the mass of the smallest object is anihilated by the corresponding one of the other object so that these two parts dissappear. What remains is the signed difference between the two.

Based upon these two fundamental operators which can be also related to the dilation and the erosion in mathematical morphology, we invented new operators which are volume invariant deformation operators : given an object shape, they can easily change this shape while keeping its volume constant:

- **the repulsion**

the repulsion operator uses a shape B to deform a shape A in such a way that the A shape gets pushed away by B . One gets such effects when modeling clay while pushing a rigid object B inside the clay mass of A.

- **the attraction**

the attraction operator, on the contrary, uses a shape B to allure the shape of A towards B. One would get such a shape starting from a clay object (shape A) and pushing it (possibly partially) with your thumb inside a mold having a shape B .

- **the separation**

the separation operator corresponds to the case when you cut the part of shape A that you used to fill up the B shape (possibly partially) in the attraction manipulation, from its main part. This way, you finish with two parts, one contained in B and the rest of A that was not used.

Now, how can we do this? The outline of the current procedure is as follows. In section **2**, we describe the morphological modeling operators which consist of the fusion operator and the difference operator . We shall show two forms of the difference operator which are denoted by the subscripts -inf and -sup respectively. It is also possible to construct other difference operators which would behave between the two limits obtained by those two. In section **3**, the detail of the fusion operation is described.

As it is the fondamental operator (all others are deduced from that one), we will describe

it in more details when compared to the others. In section **4**, after introducing negative volumes, the detail of the difference operator is shown. In section **5**, we demonstrate the performance of combinations of these modeling operators. Conclusions and future research directions are summerized in section **6**. Some properties of the morphological modeling operators are given in **Appendix**.

2 MORPHOLOGICAL MODELING OPERATORS

We propose the following modeling operators which are applied to objects A and B:

- the fusion of A and B (denoted by $A \oplus B$)
- the difference between A and B (denoted by $A \ominus B$)

The fusion and the difference operators do not commute. The result of the fusion between shapes A and B is such that it contains both A and B and has a volume which is equal to the volume of A plus the volume of B.

We propose two versions of the difference operator, the difference-inf : between A and B (denoted by $A \ominus_{inf} B$) and the difference-sup : between A and B (denoted by $A \ominus_{sup} B$). Both operate such that the volume obtained is equal to the difference between the two volumes. The specific properties of $\ominus_{inf}$ and $\ominus_{sup}$ will be discussed in section **4**. On the basis of these three modeling operators we define the following deformation operators :

- the repulsion of A by B (denoted by A^B), $A^B = (A \oplus B) \ominus B$
- the attraction of A by B (denoted by A_B), $A_B = (A \ominus_{inf} B) \oplus B$
- the separation of A by B (denoted by A|B), $A|B = (A \ominus_{sup} B) \oplus B$

The repulsion, attraction and separation operators are all idempotent :

$$(A^B)^B = A^B$$

$$(A_B)_B = A_B$$

$$(A|B)|B = A|B$$

and have some similarities with the "opening" (A^B) and "closing" (A_B and A|B) operators used in mathematical morphology [17] which lead us to call our approach "morphological".

3 THE FUSION OPERATOR ⊕

3.1 *Outline of The Method*

Let A and B be three-dimensional objects. Our aim is to create an object C such that :

- C contains A and B
- the volume of C is equal to the volume of A plus the volume of B

We suppose that each input object is a regular closed surface (otherwise, we cannot define its volume) and is described by a set of vertices and facets (polyhedral approximation). The fused object C has the same description. There are no constraints on the geometry or topolgy of A or B. They can have sharp edges and holes (this property differs from implicit function modeling).

The fused object C contains $A \cup B$. The difference between the volume of $A \cup B$ and the volume $A \oplus B$ is equal to that of $A \cap B$. The fused object C is the union of $A \cup B$ and of a layer which covers $A \cup B$, the volume of the layer being equal to $A \cap B$. In **3.2**, we introduce the fusion center which drives the direction from where the volume of $A \cap B$ will be transported to the surface of $A \cup B$. Such transport is done by scanning the 3D space around a fusion center H (see below).

Starting from objects A and B (Figure 1 : green object and red object), the steps leading to fused object C are listed below:

(1) First, we scan the 3D space around the fusion center. We then deform objects A and B, as shown in Figure 9 , to accomodate the transported volume. Their surfaces will be used to construct fused object C by simply computing the logical union between deformed A and B (discussed in section **3.3***)*.

(2) Next, we construct the intersection curve(s) between deformed objects A and B.

(3) Then, we triangulate the parts of intersecting polygons of deformed A (B), corresponding to the outside of deformed B (A). We replace the intersecting polygons by these triangles. The polygons of deformed A and B which are outside the intersection are simply merged into this shape. The

complete surface of fused object C is thus obtained as shown in Figure 1: blue object (discussed in section **3.5**).

3.2 The Fusion Center

Volume preserving fusion can be expressed in boolean operations as, the volume of $A \Upsilon B$ increased by the volume of $A \cap B$. The main idea is that we transport the shared volume $A \cap B$ to the periphery of $A \Upsilon B$. The fusion center H drives the direction from which the shared volume will be transported. The concept of a fusion center is similar to that of [16]. In the current work we can position H anywhere in the 3D space while in [16] it should be inside $A \cap B$. The shape of the fused object depends heavily on H so that it is, in fact, a very powerful tool. This is illustrated in Figure 7. An application of this effect is presented in figure 8 where a human head corresponds to object A. We put an ellipsoid B inside A and put H on the right of B so that the face gets an inflated left cheek exactly as when you do it yourself when inflating air in your mouth and orient it with your muscles (here with H); if H is put on the left of B, it is the right cheek which becomes inflated (see top right of Figure 8). If you put it behind B, it is the mouth and the bottom of the face which becomes now inflated (see bottom left of Figure 8). Another interesting effect is produced on bottom right of Figure 8 by replacing the ellipsoid by a parallepipedron.You may put the ellipsoid out of the face with a small inclusion inside the mouth to have the face blow a balloon out of her cheek. So , here with the simple play on H (you may move also B a bit in order to produce a perfect aspect) you may obtain an interesting animation. In order to feel better the possibilities offered by the H displacement, we show in the 2D case in figure 7, a variety of ways in which volume can be distributed around the surface. The volume which is triggered by H is shown in yellow and the deformation produced on A and/or B is colored in green. The result of the fusion is the total outside shape. When H is set in the intersection, the excess of volume is spread out all over the union of A and B, which makes a much smoother result. When it is set outside the intersection, it permits to produce sharp edges and deform only a part of the union between A and B in a controled manner. Due to this enhanced flexibiilty the $\oplus$ operator should be more accurately written by $\oplus_H$. However

for simplicity we shall simply refer to the operator as $\oplus$.

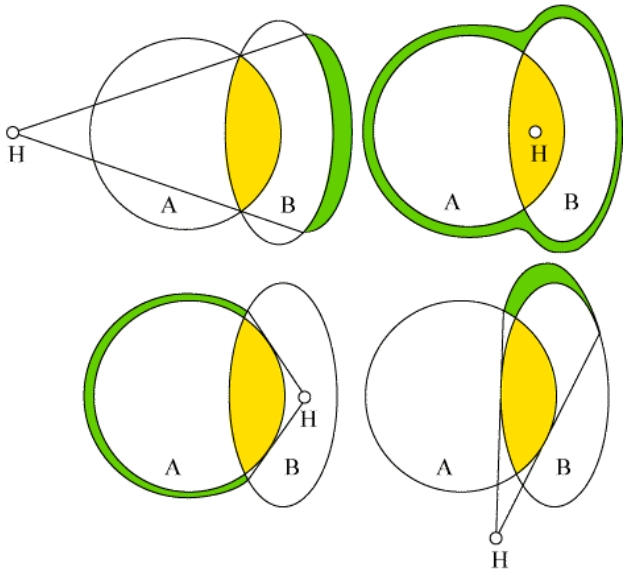

Figure 7: Influence of the position of the fusion center H on the displacement of volume of $A \mathbin{I} B$ (yellow) at the periphery of $A \mathbin{Y} B$ (green).

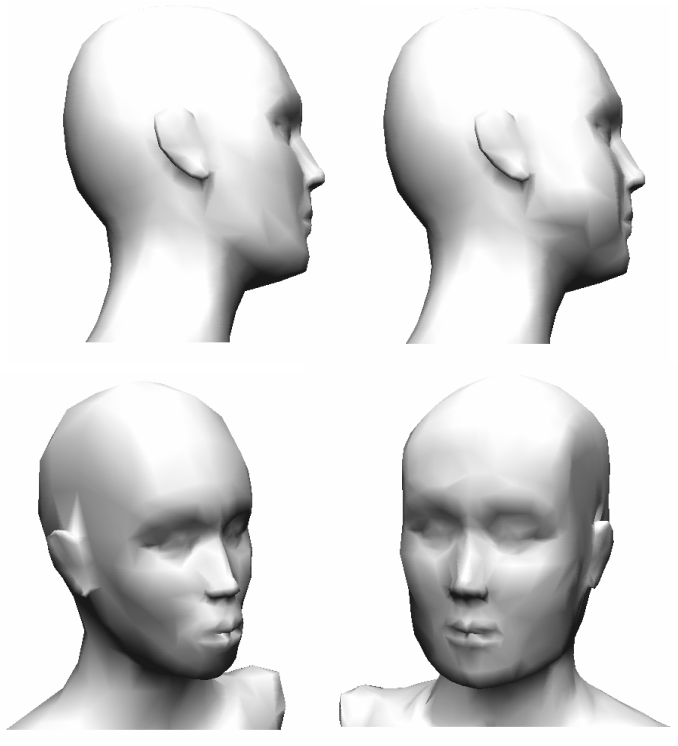

Figure 8: Possibilities offered by manipulations of H

3.3 Interval Composition and Construction of the Surface

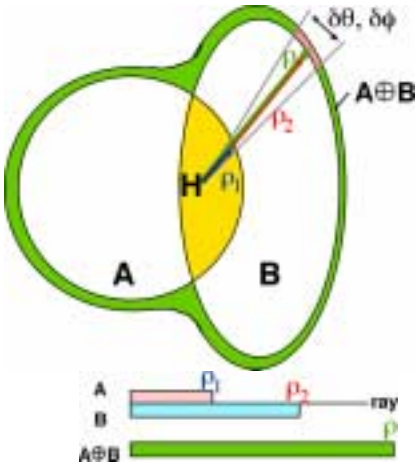

Figure 9: Example of how the shared volume $A \cap B$ is locally transported to the outside of $A \cup B$ (from [16]). See formula (1).

The surface of the fused object can be obtained as follows:

We scan the 3D space around H by infinitesimal cones in spherical coordinates (θ, ϕ); the volume of $A \cap B$ is transported to the closest free space available outside of $A \cup B$ as illustrated in Figure 9.

In spherical coordinates around H, the volume of a cone of height $\rho(\theta, \phi)$ is equal to $1/3\ \rho^3\ \delta\theta\delta\phi$. The cone of height $\rho_1(\theta, \phi)$ belonging to $A \cap B$ and $\rho_2(\theta, \phi)$ belonging to B (or A) , will produce a local fusion of A and B which brings the fused surface to $\rho(\theta, \phi)$ such that:

$$\rho(\theta, \phi) = \sqrt[3]{\rho_1(\theta, \phi)^3 + \rho_2(\theta, \phi)^3} \qquad (1)$$

Previous work [16], started from a simple object (i.e. tetrahedron) which includes H inside, formula (1) was applied for each vertex. Each vertex was then displaced to the point at a distance of $\rho(\theta, \phi)$ from H in direction (θ, ϕ). Polygons of the object were then subdivided and formula (1) was applied for the adapted vertices again. This procedure was continued until the curvature becomes larger than a given threshold. This technique required that the fusion center H should be inside $A \cap B$ and the objects should be star-shaped. The resultant number of polygons and vertices obtained depended on the threshold controling the curvature.

These restrictions can be avoided by deforming the input graphs of A and B, which allows to keep the control of the surface obtained. We compute the deformation of A by B, the deformation of B by A. The result of the fusion is locally (among the two possibilities, for each tube) the solution which contains the other one. It is thus, the union of deformed A and deformed B.

The procedure is : draw a ray starting from H and hitting each vertex V of object A, determine all intersecting intervals with A and B , as it is done in conventional ray tracing [25]. This is illustrated in Figure 10. At the point where the ray is exiting the volume modify its location due to the transport of volume between the objects via Equation (1). Volume is transported as follows. First, compute $A \Upsilon B$ (light blue), $A \cap B$ (yellow) and the free space $\overline{A \Upsilon B}$ (purple) between the vertex V and the fusion center H. For illustration purposes we will not consider what is outside location V even if there are still other A and(or) B intervals due to complex folding of the objects and we assume that the space is empty after location V. In other words the vextex V denotes the outmost vertex of our demonstration object.

The volume of each $A \cap B$ interval is transported to the nearest available free space interval located between itself and V. If the volume of free space is smaller than that of $A \cap B$ (case of (b) in Figure 10), the free space is occupied and the difference between the volume of $A \cap B$ and the free space is transported to the next available free space, and this procedure is iterated until all the volume of $A \cap B$ is placed.

Finally, when all intersection intervals have been treated, we determine the displacement of the vextex V to V' which is such that the interval VV' corresponds to the amount of volume of the intersection $A \cap B$ which has still not been placed in the available free space between H and V. If the ray is getting IN the volume at location V, do not move point V. The same operation is then performed similarily for all vertices of B.

Remark: if the space after location V is occupied by A intervals and VV' intersects some of them, the case will be treated by the self-intersection procedure explained below. If the deformation of B locally passes V' (for example, if a B interval goes further than V, and is containing V), V' will be simply deleted later by the computation of the union

of deformed A and deformed B.

Figure 10 shows two examples of interval composition in the fusion case. The result of such a fusion is shown in Figure 1, when all rays were treated.

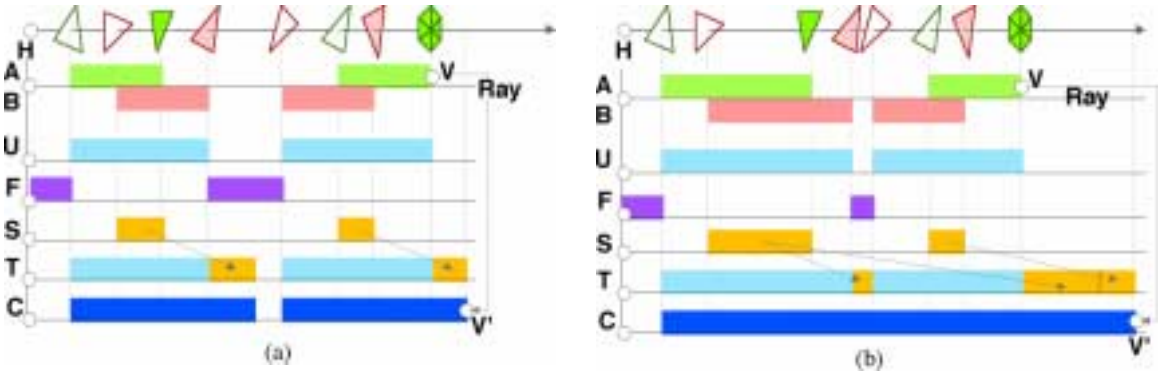

A: interval occupied by object A (in green) along the ray

B: interval occupied by object B (in red) along the ray

U: interval occupied by $A \vee B$ (light blue)

F: interval occupied by free space (purple)

S: interval occupied by shared volume ($A \wedge B$)

T: Transport of the shared volume in the free space

C: fused object (dark blue)

Figure 10: Two examples of interval composition in the case of the fusion operator. Shaded triangles denote surfaces at which the ray from H exits volume A (green) and volume B(red). V is the vertex of A which is considered and the only one which will be displaced. We also show the displacement of V to V' . In case (a) the shared volume is smaller than the free space. In case (b) it is bigger than the free space; the difference between the shared volume and the volume of free space already used is transported to the next available free space interval.

In general we keep the same graph for A and B, but simply the locations of the vertices are displaced. An exception occurs when there are self-intersections. Self-intersections are possible as we deal with general surfaces as illustrated in figure 11. The problem of self-intersection is solved using the intersection procedure

explained in **3.4** (for A intersecting B). We compute the intersection curves and produce the modified graph of A (or B), which includes this curve, and delete all inside polygons of A (or B).

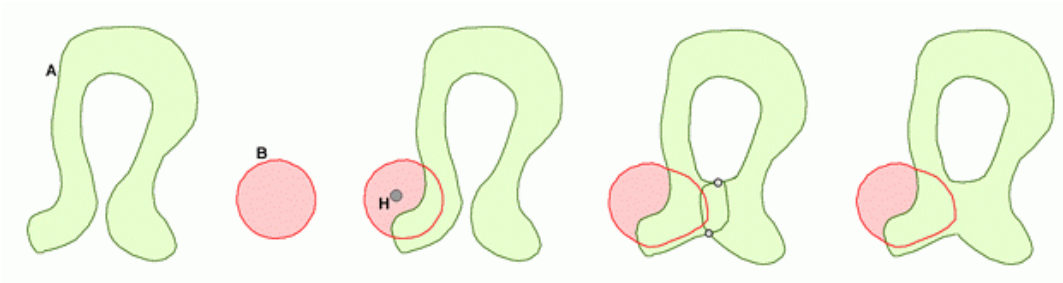

(a) **(b)** **(c)** **(d)**

Figure 11. Procedure used in the case of self-intersection.

(a) input object A and B,

(b) positioning of B and H around A for a future fusion

(c) deformation of A and B showing the connected outside surface (in A)

(d) internal polygons of the self-intersection volume are eliminated

It is interesting to note that the fusion of A and B can have a topology which differs drastically from those of A and B.

3.4 Construction of the Intersection Between Deformed A and B

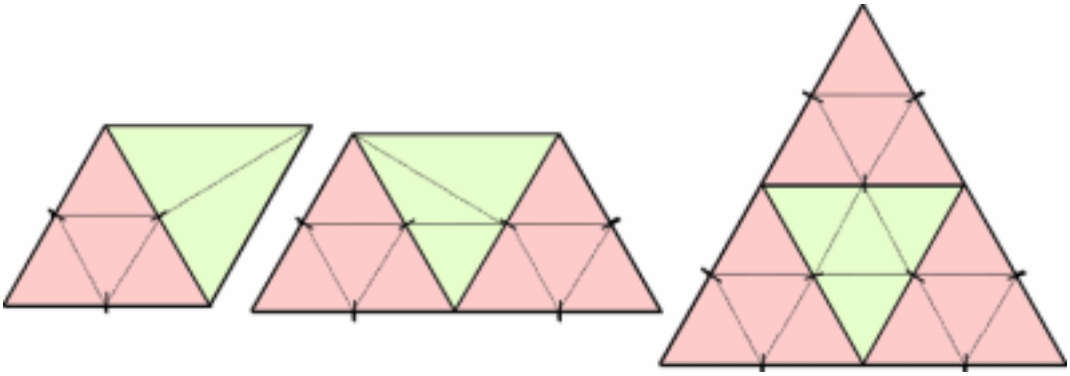

Figure 12. One level of subdivision of an intersecting triangle (red) and *corresponding* subdivision for neighboring ones (green).

Object C is the union of deformed A and deformed B. The technique used is classical, and based upon *[20], [24].*

In order to obtain a more precise fusion, refining the intersection zone might be useful. We first subdivide the intersecting triangles. In order to avoid T-junctions (which break the closed surface property), the neighboring triangles should be also subdivided. It is done for the three possible schemes shown in Figure 12.

4 DIFFERENCE OPERATOR ⊖

We now propose a type of "dual" operator to fusion: given two shapes A and B, we construct a shape C = A⊖B such that the volume of C is equal to the volume of A minus the volume of B. In order to do so, we authorize negative volumes (masses) with the assumption (as in astrophysics) that negative and positive mass cannot coexist in the same portion of space. As for the fusion case, the operation is performed with respect to a center of fusion/difference H.

- If A and B do not intersect, then A⊖B is simply A (with positive volume) and B with negative volume.
- If B is inside A, it is simply the logical operator (A – B).
- If A and B intersect, we propose two different operators $A\ominus_{inf}B$ and $A\ominus_{sup}B$ (which perform both the same operation in the two former situations).

The properties of $\ominus_{inf}$ and $\ominus_{sup}$ are such that:

-The result of $A\ominus_{inf}B$ is the closest to B when the volume of the result is positive, and the furthest from A when the volume of the result is negative (as illustrated in Figure 13).

-The result of $A\ominus_{sup}B$ is the furthest from B when the volume of the result is positive and the closest to A when the volume of the result is negative (as illustrated in Figure 15).

As in the fusion case, we consider small cones around H. Having considered volume constraints, we have to solve mainly a 1D interval composition operation. We describe the interval composition of the difference operators in sections **4.1** and **4.2**. The 3D result is obtained by applying the former interval compositions and by using the proper boolean operation on the deformed objects in a similar manner to the fusion case.

4.1 Difference Operator $A \ominus_{inf} B$

The property of the $\ominus_{inf}$ operator is that the result of $A \ominus_{inf} B$ is the closest to B (which has a negative weight) when the volume of A is bigger than the volume of B, that is, when the result is a positive volume. In the other case (the volume of A smaller than the volume of B) the result obtained is the furthest from A, which also means that it is the closest to B (algebrically).

The interval composition depending on the relative sign and positions of A and B (there are 5 cases) is presented in Figure 13. The bars represent the intervals occupied by A or B, and the results are shown as light blue(positive) or green(negative) intervals. On the left, the A interval is bigger than the B interval and the result is a positive interval. When A and B intersect, the interval $A \cap B$ is set to zero. The rest (or part of the rest) of the B volume and the similar A part (annihilated by B) are presented in red. On the right of Figure 13, we treat the case when A interval is smaller than B interval; we use the same procedure and the same color conventions. The result is presented in green (negative volume). Figure 14 presents the result of this composition in the 2D case.

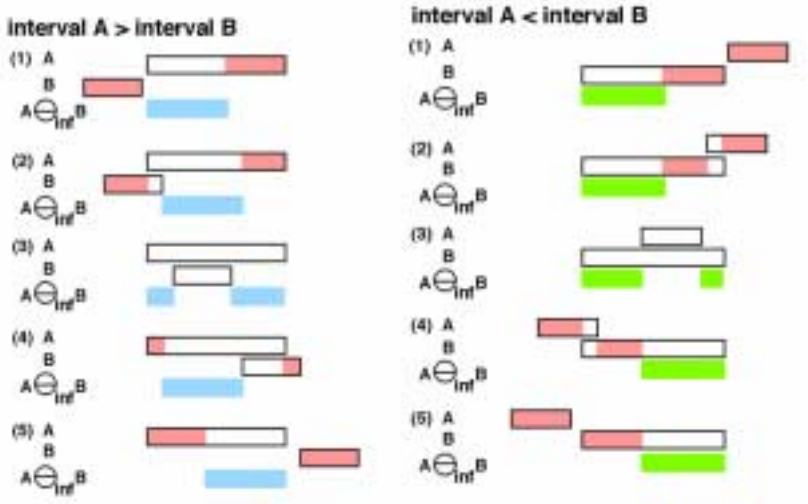

Figure 13: Interval composition rule for the construction of $A \ominus_{inf} B$. Positive results are shown in blue, negative one in green. The red parts are those of A and B which were mutually destroyed. The white parts are the parts of A or B which were either destroyed as intersecting parts or remained untouched. The result is the closest to B when interval of A is bigger than that of B, and furthest from A when interval of A is smaller than B.

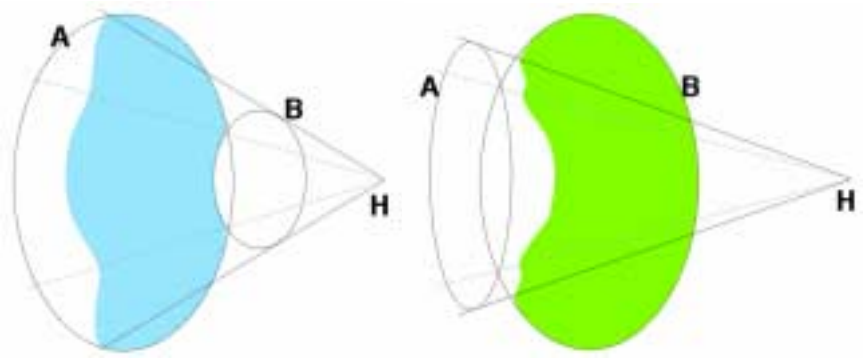

Figure 14: 2D results of $A \ominus_{inf} B$ composition.

We have to point out that in cases (1) and (5) of Figure 13, the volume transfer is performed (in red), though A and B intervals are disconnected, but we know that globally A volume and B volume intersect (difference with the first case of the previous paragraph).

$A \ominus_{inf} B$ can be visualized either when the result is positive (case of volume of A bigger than volume of B) but also when it is negative (volume of A smaller than volume of B): we simply visualize it in a dual (negative) subspace, so that both cases are useful for object modeling.

4.2 Difference Operator $A \ominus_{sup} B$

We are once again in the case when A and B intersect globally. This other difference operator is such that the result of $A \ominus_{sup} B$ is the furthest from B when volume A is bigger than B, and closest to A when the volume of A is smaller than B (which also means that it is the furthest from B algebraically). Figure 16 shows a 2D result of the $A \ominus_{sup} B$ composition similarly to Figure 14 for $A \ominus_{inf} B$. The interval composition is presented in Figure 15 (we use the same color conventions as in Figure 13) . We can verify that the interval results are different from those of Figure 13.

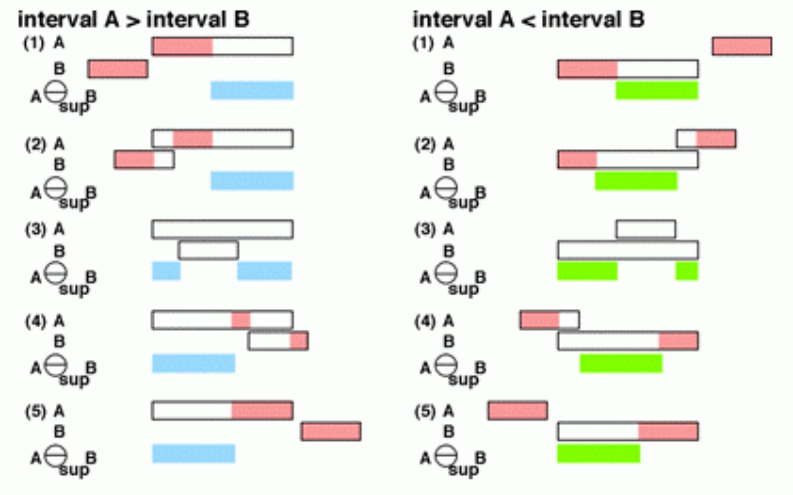

Figure 15. Interval composition rules for the construction of $A \ominus_{sup} B$. The result is the furthest from B when the interval of A is bigger than that of B, and closest to A when the interval of A is smaller than B.

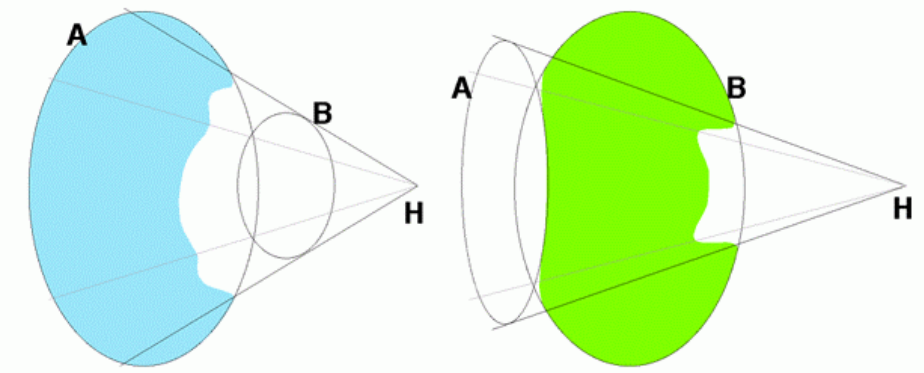

Figure 16: 2D results of the $A \ominus_{sup} B$ composition.

5. OBJECT DEFORMATION BY OPERATOR COMBINATIONS

It is possible to use the three former operators $\oplus$, $\ominus_{inf}$, $\ominus_{sup}$ to produce new shape deformations which have the properties of keeping the volume constant.

5.1 The Repulsion Operator $(A \oplus B) \ominus B$

Given a center of composition H (as before) we define the repulsion of A by B (denoted by A^B) by the following operator:

$$A^B = (A \oplus B) \ominus B$$

As $A \oplus B$ contains B, there is only one type of difference, which is obtained by a logical operation. It is clear that the volume of A^B is equal to that of A. The behavior of a repulsion operator is visualized in Figure 4 (input objects (red and green) and result (blue)). Note that the repulsion operator works independently of the choice of the type of subtraction operator (therefore no subscript is listed above).

The behaviour of the repulsion operator can be described by the effect produced by a hard tool B which is crushed on a piece of clay of shape A. The clay deforms itself around the tool B. This behaviour is obtained for any shapes A and B.

The graph of the repulsion surface result is simply obtained from the graph of $A \oplus B$ where outside triangles of B are replaced by inside ones, inside ones by outside ones and intersection between A and B done similarily as in $A \oplus B$.

5.2 The Attraction Operator $(A \ominus_{inf} B) \oplus B$

The attraction of A by B (denoted by A_B) is :

$$A_B = (A \ominus_{inf} B) \oplus B$$

The volume of A_B is also equal to that of A. Here again, B is a deformation tool which attracts the volume of A to itself (depending on H). An example of attraction is shown in Figure 3 (input objects (red and green) and result (blue)).

5.3 The Separation Operator $(A \ominus_{sup} B) \oplus B$

The separation of A by B (denoted by A|B) is :

$$A \mid B = (A \ominus_{sup} B) \oplus B$$

B attracts the shape of A so strongly that it pulls a part of volume of A out of it. We believe that this operator has a lot of potential in order to model cell divisions as in genetics. An example of separation operator is produced in Figure 5.

5.4 Volume Preserving 3D Morphing

We want to produce the metamorphosis of object A to object B. As before, this operation is performed relative to a morphing center H. We often choose H as being the center of gravity of both A and B. If the volume of A is not equal to the volume of B

(suppose volume of A is bigger than volume of B), we first compute a similarity factors:

$$s = \sqrt[3]{\frac{V_A - V_B}{V_A}}$$ where V_A is the volume of A and V_B the volume of B

and we perform the similarity of center H and facter s on A so that the volume of A becomes the same as that of B. (We use the same basic idea as in [9, 10]).

Then we apply the fusion operation to :

$$C(t) = ((1 - t)^{1/3} * A) \quad ((t)^{1/3} * B) \qquad (2)$$

and we vary t from 0 to 1 (as in [16]).

This operation is such that the volume of C(t) is always equal to the volume of A (normalized) or B. The important difference with [16] is that we can apply this morphing for any pair of A and B shapes (see Figure 6).

If we do not normalize the objects, 3D morphing using (2) is such that the volume of C(t) varies linearly from that of A (t=0) to that of B(t=1).

6 CONCLUSIONS AND FUTURE WORK

We proposed a new set of functions allowing modeling and animation of deformable objects. The functions are quite easy to use. We first define a composition center and choose two input objects. The composition is then performed automatically. It is possible to produce animations while moving the composition center and/or the input objects. Since the functions keep the global volume of the objects constant, resulting animations produce an impression of realism even when the shapes of input objects are simple.

The functions presented here require about 20 seconds (1000 polygons, 500 vertices for each input object) of CPU time to be computed on a Silicon Graphics Maximum Impact (R10000) and about 1 minute on a Power Macintosh (PPC604/132MHz).

Of course, a lot of work has still to be done. First, using various combinations of morphological operators seems to be powerful. Taking into account material properties (diffuse, ambient, specular, transparency etc.) is also important. Texture fusion

might also be challenging. Another direction of extension of our work is to consider not only a composition center H, but also many of them, describing a line, a curve, or even a surface.

REFERENCES

[1] D.R.Forsey, R.H.Bartels. "Hierarchical B-Spline Refinement" Proc. SIGGRAPH '88 (Atlanta, Georgia, Aug 1-5, 1988). In Computer Graphics Proceedings, 22, pp. 205-212.

[2] P.Borrel, D.Bechmann. "Deformation of n-Dimensional Objects" In Symposium on Solid Modeling Foundations and CAD/CAM Applications, pp. 351-369, June 1991.

[3] B.S.Cobb. "Design of Sculptured Surfaces Using the B-Spline Representation" PhD thesis, University of Utah, June 1984.

[4] S.Coquillart. "EFFD: A Sculpturing Tool for 3D Geometric Modeling" Proc. SIGGRAPH '90 (Dallas, Texas, Aug 6-10, 1990). In Computer Graphics Proceedings, 24, pp. 187-196.

[5] T.W.Sederberg, E.Greenwood. "A Physically Based Approach to 2D Shape Blending" Proc. SIGGRAPH '92 (Chicago, Illinois, July 26-31, 1992). In Computer Graphics Proceedings, 26, pp. 25-34.

[6] C.Hoffmann, J.Hopcroft. "The Potential Method for Blending Surfaces and Corners" In G.Farin editor, Geometric Modeling: Algorithms and New Trends, pp. 347-365, SIAM, Philadelphia, 1987.

[7] J.F.Hughes. "Scheduled Fourier Volume Morphing" Proc. SIGGRAPH '92 (Chicago, Illinois, July 26-31, 1992). In Computer Graphics Proceedings, 26, pp. 43-46.

[8] S.Coquillart, P.Jancene. "Animated free-form deformation: An interactive animation technique" Proc. SIGGRAPH '91 (Las Vegas, Jul 28 - Aug 2, 1991). In Computer Graphics Proceedings, 25, pp. 23-26.

[9] A.Kaul, J.Rossignac. "Solid-interpolating Deformations: Construction and Animation of PIPs" In Proc. Eurographics '91, pp. 493-505, September 1991.

[10] J.R.Kent, W.E.Carlson, R.E.Parent. "Shape Transformation for Polyhedral Objects"Proc. SIGGRAPH '92 (Chicago, Illinois, July 26-31, 1992). In Computer

Graphics Proceedings, 26, pp. 47-54.

[11] T.W.Sederberg, S.R.Parry. "Free-Form Deformation of Solid Geometric Models" Proc. SIGGRAPH '86 (Dallas, Texas, Aug 18-22, 1986) In Computer Graphics Proceedings, 20, pp. 151-160.

[12] R.Szeliski, D.Tonnesen. "Surface Modeling with Oriented Particle Systems" Proc. SIGGRAPH '92 (Chicago, Illinois, July 26-31, 1992). In Computer Graphics Proceedings, 26, pp. 185-194.

[13] B.Wyvill, C.McPheeters. "Animating Soft Objects" In The Visual Computer, volume 2, pp. 235-242, 1986.

[14] B.Wyvill, J.Bloomenthal, T.Beier, J.Blinn, A.Rockwood. "Modeling and Animating with Implicit Surfaces" In Siggraph Course Notes, volume 23, 1990.

[15] G.Wyvill, C.McPheeters, B.Wyvill. "Data Structure for Soft Objects" In The Visual Computer, volume 2, pp. 235-242, Springer Verlag 1986.

[16] P.Decaudin, A.Gagalowicz. "Fusion of 3D shapes" In Fifth Eurographics Workshop on Animation and Simulation, Oslo, Norway, September 1994.

[17] J.Serra, “Image Analysis and Mathematical Morphology”, Academic Press, New York 1982.

[18] E. L. Lloyd, "On Triangulations of a Set of Points in the Plane", Proc. 18th Annu. IEEE Sympos. Found. Comput. Sci., pp.228-240, 1977.

[19] T. Nishita and E. Nakamae, "A Method for Displaying Metaballs by using Bezier Clipping, Computer Graphics Forum, "Eurographics '94 Conference issue", volume 13, Eurographics, Basil Blackwell Ltd, pp.271-280.

[20] C.M.Hoffmann, "Geometric and Solid Modeling. An Introduction", Morgan Kaufmann, California, 1989.

[21] A.Lerios, C.D.Garfinkle, M.Levoy "Feature-Based Volume Metamorphosis", Proc. SIGGRAPH '95 (LosAngeles, California, Aug 6-11, 1995). In Computer Graphics Proceedings, pp.449-456.

[22] Takushi Fujita and Katsuhiko Hirota and Kouichi Murakami, "Representation of Splashing Water Using Metaball Model (in Japanese)", Fujitsu volume 41, pp.159-165, 1990

[23] Jianhua Shen and Daniel Thalmann, "Interactive Shape Design Using Metaballs and Splines", Implicit Surfaces '95, 1995.

[24] D.H.Laidlaw, W.B.Trumbore, J.F.Hughes, "Constructive Solid Geometry for Polyhedral Objects", Proc. SIGGRAPH'86 (Dallas, Texas, Aug 18-22), pp.161-170.

[25] S.D.Roth, "Ray Casting for Modeling Solids", Computer Graphics and Image Processing volume 18, pp.109-144, 1982.

[26] K.Weiler, P.Atherton, “Hidden Surface Removal Using Polygon Area Sorting”, Computer Graphics volume 11, pp.214, 1977.

Appendix: Relation Between $A\ominus_{inf} B$ and $A\ominus_{sup} B$

It happens that both operators are dual (as erosion and dilatation in mathematical morphology). If we take the dual of $A\ominus_{inf} B$, that we denote $\overline{A\ominus_{inf} B}$, (it corresponds to simply changing the sign of the volume), we see that $A\ominus_{inf} B$, when $B < A$, (and when the sign of the result is changed) corresponds exactly to the case $B\ominus_{sup} A$, $A < B$. Similarily $A\ominus_{inf} B$, $A < B$ corresponds to $B\ominus_{sup} A$, $B < A$ (compare Figures 13 and 15). This way we obtain the very interesting duality relations:

$$\overline{A\ominus_{inf} B} = B\ominus_{sup} A$$

$$\overline{A\ominus_{sup} B} = B\ominus_{inf} A$$

The dual of a shape (sign volume inversion) can be also interpreted as $\ominus$ shape (as there is no difference between $\ominus_{inf}$ and $\ominus_{sup}$), so that we have :

$$\ominus A\ominus_{inf} B = B\ominus_{sup} A$$

$$\ominus A\ominus_{sup} B = B\ominus_{inf} A$$

These relations mainly express the fact that if you visualize a negative volume coming from the difference between two shapes A and B, this volume looks the same as the positive volume of B minus A.